SUPPLEMENTARY METHODS

CDP library construction

CDP libraries were cloned into mammalian surface display lentivector SDGF, including error-prone PCR mutagenesis for diversity libraries, as previously described *(62)*, sourcing our CDP pools as ssDNA oligomers from Twist Bioscience and our singleton CDP genes as dsDNA from IDT. CDP quality assays used the SDPR vector, while all CDPs used for target-binding screening or assessment were cloned into the SDGF vector. Experiments involving pooled analysis proceeded 3-4 days after transduction of lentiviral libraries into 293F (ThermoFisher R79007) cells at multiplicity of infection (MOI) ≈ 1, while singleton candidate analysis proceeded 2-3 days after transient transfection of 2.5 μg SDGF plasmid into 1 million 293F cells.

Flow cytometry

Mammalian display cell staining experiments were all variations on those previously described *(62)*. SDPR CDP quality assays used anti-His-iFluor 647 antibodies (Genscript A01802), staining using identical protocols to those used previously *(10, 62)*. For surface quality scoring (Fig. 2C), quantitation of performance was performed using deep sequencing and 4-way sort binning of cells with varying anti-6xHis staining as described previously *(10, 62)*. For PD-L1 screens using MY-Con, NCL2, or DEMYS libraries, cells were stained at 200 nM biotinylated, 6xHis-tagged PD-L1 (Acro Biosystems PD1-H82E5). Each screen began with magnetic sorting (either Miltenyi AutoMACS with anti-biotin microbeads [Miltenyi 130-090-485] or STEMCELL EasySep Big Easy magnet with EasySep Release Human Biotin Positive Selection Kit [STEMCELL 17653]) of 500 million cells transduced 3-4 days prior with lentivirus at MOI ≈ 1, using PD-L1 in place of an antibody and PBS + 3% BSA and 2 mM EDTA as the cell incubation buffer but otherwise as per manufacturer's recommendations (EasySep) or as previously described *(30, 62)* (AutoMACS). Subsequent sorts involved resuspending up to 24 million cells in 3 mL Flow Buffer (PBS + 0.5% BSA and 2 mM EDTA) containing 200 nM PD-L1 and either 200 nM streptavidin-AlexaFluor 647 (ThermoFisher S21374) or 200 nM anti-6xHis for 30 mins on ice. Three volumes of Flow Buffer were then added, after which cells were pelleted and resuspended in Flow Buffer for flow sorting. SSM screening involved no magnetic sorting and two rounds of flow sorting, where staining was as above except for using 4 nM PD-L1 and 4 nM streptavidin-AlexaFluor 647 and also including an additional 3 mL Flow Buffer rinse after staining before final pelleting and resuspension for sorting. Flow sorting took place on an Aria 2 (Becton Dickson), collecting about 300,000 cells per round of sorting. Cell staining experiments for simple analysis used identical staining protocols to the sorting, except PD-L1 and streptavidin-AlexaFluor 647 concentrations were reduced to 40 nM.

Protein-specific recombinant protein production and QC

CDP purification from media: CDPs were secreted fused to an N-terminal siderocalin carrier protein which was separated via a tobacco etch virus (TEV) protease recognition site and TEV protease (1 mg TEV per 20 mg protein) prior to an additional reverse phase chromatography step (AKTA Pure, GE Healthcare) to remove the free siderocalin and uncleaved fusion protein. Purified CDPs were frozen at -80°C and lyophilized. Protein content of aliquots were quantitated via amino acid analysis (AAA Service Laboratory Inc.).

PD-L1, PD-1-Fc, Control-Fc, and BTTC purification from media: Non-CDP recombinant proteins were spin-concentrated (Amicon Ultra 30 kDa columns) and purified by

size exclusion chromatography (HiLoad Superdex 26/600, Cytiva 28989336), buffer-exchanging into PBS in the process. Protein-containing fractions were pooled, concentrated, brought to 5% glycerol and flash-frozen with liquid N_2. Aliquots were stored at -80°C.

CDP QC: Purified CDP lyophilates were resuspended in water to 1 mg/mL, followed by dilution with 1x PBS to a final concentration of 0.5 mg/mL in 0.5x PBS. CDP solutions were filtered (0.22 μm, Millipore UFC30GVNB) prior to HPLC/MS analysis. 25 μL of the filtrate was injected onto an Agilent 1260 Infinity instrument with inline 6120 Quadrupole MS using an Agilent Poroshell 120 SB-C18 column (PN 687975-902T). CDPs were eluted using a gradient of water + 0.1% TFA (Buffer A) and acetonitrile + 0.1% TFA (Buffer B), ramping from 5% Buffer A / 95% Buffer B to 45% Buffer A / 55% Buffer B over 10 min with a flow rate of 2 mL/min. MS was analyzed through use of the "Select Spectrum at Apex Position" tool within the Agilent Chemstation software and selecting the major product present in the RP chromatogram. Resulting MS spectra and the major m/z peaks were compared to theoretical mass calculations (Expasy).

CDP structural modeling

All custom scripts for parsing outputs of I-TASSER and Rosetta software packages are available upon request. CDP structures were modeled by first running I-TASSER v5.1 in fast mode (-light true) with all other command line options left as default. An example command is below:

$pkgdir/I-TASSERmod/runI-TASSER.pl -pkgdir /home/[yourname]/I-TASSER5.0/I-TASSER5.1 -libdir /home/[yourname]/ITLIB/ -seqname [sequence_name] -datadir ./ -usrname $USER -runstyle parallel -light true

Output PDB files were re-oriented so their coordinates centered on the origin using a custom script. Re-oriented PDB files were then fed into a custom script to calculate all pairwise distances between the cysteine CB atoms and arrive at the pairing (e.g. 1-4, 2-5, 3-6) whose summed CB-CB distances are the smallest. This set of proposed Cys-Cys pairings and the I-TASSER model were then processed in Rosetta (MPI version 2017.52.59948) using a ForceDisulfides mover followed by backbone and side chain minimization using a MinMove mover. XML input file is as follows:

```
<ROSETTASCRIPTS>
  <SCOREFXNS>
    <ScoreFunction name="r15_cart" weights="ref2015" >
      <Reweight scoretype="pro_close" weight="0.0" />
      <Reweight scoretype="cart_bonded" weight="0.625" />
    </ScoreFunction>
  </SCOREFXNS>
  <RESIDUE_SELECTORS>
  </RESIDUE_SELECTORS>
  <TASKOPERATIONS>
```

```
        </TASKOPERATIONS>
        <FILTERS>
        </FILTERS>
        <MOVERS>
          <MinMover name="min_cart" scorefxn="r15_cart" chi="true" bb="1" cartesian="T"
/>
            <ForceDisulfides name="force_ds" scorefxn="r15_cart"
disulfides="%%pairings%%"/>
        </MOVERS>
        <APPLY_TO_POSE>
        </APPLY_TO_POSE>
        <PROTOCOLS>
          <Add mover="force_ds" />
            <Add mover="min_cart" />
        </PROTOCOLS>
        <OUTPUT scorefxn="r15_cart" />


</ROSETTASCRIPTS>
```

Outputs were used as CDP structural models for downstream analysis and docking experiments.

Low-resolution CDP docking

CDP models were assessed for target docking using Rosetta (MPI version 2017.52.59948). First, STRIDE software (using a custom script available upon request) was run on the input CDP model to determine whether an unstructured region is present. This was done because CDPs often have unstructured regions between cystines that should not be interpreted as rigid for the purposes of docking. The bounds of these unstructured loops (in the form of a file called "loops.txt") are then fed, along with the model, into Rosetta using the FloppyTail application. Sample Rosetta command line input is as follows:

```
$ROSETTA/rosetta_bin_linux_2017.52.59948_bundle/main/source/bin/FloppyTail.static.linuxg
ccrelease -s ${original_ligand} -in:file:movemap loops.txt -overwrite -ex1 -ex2 -
packing:repack_only -FloppyTail:shear_on 0 -FloppyTail:refine_repack_cycles 30 -
FloppyTail:perturb_cycles 5000 -FloppyTail:refine_cycles 30 -out:suffix _loopflop -nstruct 20
```

20 "loopflop" models that represent loop perturbations were generated when loops were present. The script and inputs were calibrated to resemble the conformers of an NMR ensemble. The loopflop models (or single input if no loops were apparent) were then combined with the target structure (sourced from an RCSB PDB) into a single PDB file and fed into Rosetta's docking

protocol RosettaDock in low resolution mode. Sample Rosetta command line input is as follows:

$ROSETTA/rosetta_bin_linux_2017.52.59948_bundle/main/source/bin/docking_protocol.static.linuxgccrelease -in:file:s [complex.pdb] -nstruct [100 or 2000] -partners B_A -dock_pert 3 8 -spin -randomize1 -randomize2 -ex1 -ex2aro -low_res_protocol_only -out:file:silent ${scaffold}_${target}_lowresdock.silent -out:file:scorefile score_global_dock.sc -out:suffix _global_dock

When loopflop models were used, 100 docks per loopflop model were created ("-nstruct 100"). When the original model (no loops found) was used, 2000 docks were created ("-nstruct 2000"). For most targets, the 100 lowest energy docks (among which no more than 20 per loopflop model could be used) were collected, and the center of mass of the CDP calculated for each dock. DBSCAN clustering (part of the scikit-learn Python module) was performed on these top 100 centers-of-mass with a maximum distance of 8 and minimum cluster size of 10 (all other options/metrics were default). Members of clusters identified by DBSCAN were used to identify the geometric center of the cluster, which was assigned as a possible docking site for that CDP. Candidate docking sites of multiple CDPs were also analyzed by DBSCAN clustering to identify regions that appeared especially permissive to CDP low resolution docking. For this, all proposed docking sites for all analyzed CDP models from NCL2 were used for DBSCAN cluster analysis, with a maximum distance of 2 and a minimum cluster size of 10 (all other options/metrics were default). The top-scoring CDP centers of mass within each cluster (up to 200) were visualized in PyMol as spherical pseudoatoms, and the cluster itself was visualized as a mesh surface over these clustered pseudoatoms. The CDPs within each cluster, ranked by the lowest average dock energy, could then be used for the construction of docking-enriched DEMYS libraries. This was done with CDPs whose predicted docking sites to PD-L1 were closest to the PD-1 binding site (using PDB 4ZQK).

Crystallization and crystallography

CDPs used in model-vs-crystal analysis that were previously published include PDBs 6AY8, 6ATY, 6ATM, 6AVA, 6AV8, 6AUP, 6AVC, 6AVD, 6ATL, 6ATN, 6ATS, 6ATW, 6ATU, and 6AY7. Please refer to their associated publications *(6, 22)* for their crystallization conditions and for data collection and refinement methods. Methods associated with novel CDP structures are described here.

CDP crystallography: Protein preparation and crystallization were performed as described *(6)*. In brief, lyophilized protein samples were resuspended in 25 mM PIPES pH 7.2, 150mM NaCl, 1mM EDTA and 0.02% sodium azide buffer at ~80 mg/mL. A TTPLabTech mosquito robot was used to set up high-throughput crystallization screenings a sitting-drop vapor-diffusion method at room temperature in 96-well plates (TTP Labtech Ltd, UK). Initial screening was done using Nextal broad matrix crystal screening condition of JCSG+ Suite, PEGs Suite, and AmSO4 Suite (Qiagen) with 1:1 protein solution to reservoir solution mix. Crystals grew in various conditions as listed in table S1. Crystals were looped from screening plates and cryopreserved in reservoir solution supplemented with 15% v/v glycerol.

Diffraction data were collected using Cu K-α X-ray source. Crystals were mounted in arbitrary orientations and collected at cryogenic temperatures. Diffraction data were collected in a single continuous scan. Single crystals were used to collect highly redundant data (table S1).

Data were reduced and scaled using HKL2000 *(65)*. Initial phases were determined by molecular replacement using PHASER *(66)* in the CCP4 program suite *(67)* using x-ray crystallography structure for the Protease Inhibitor LCMI II, PDB code 1GL1 *(68)* as the search model. Iterative cycles of model building and refinement were performed using COOT *(69)* and REFMAC *(70)*. Structure validation was performed using MolProbity *(71)*. The structures were deposited into the RCSB *(72)*, accession codes PDB 7SGQ, 7SLT, 7SAO, 7SNC, 7SND, and 7SAP.

PDL1B1G2-N22Q:PD-L1 co-crystallography: The N-terminal extracellular domain of PDL1 was expressed in HEK293 cells as a fusion protein with human siderocalin separated by a TEV cleavage sequence; it was purified as described in the Methods. PDL1B1G2-N22Q was reconstituted from a lyophilized powder in 1x PBS. The complex was isolated by size exclusion chromatography in crystallization buffer (12 mM PIPES pH 7.2, 150 mM NaCl, 1 mM EDTA) and concentrated to ~10 mg/ml. Initial crystals were obtained by vapor diffusion over well solutions of 200 mM potassium citrate and 2.2 M ammonium sulfate. The crystals were improved through multiple rounds of macro seeding into drops of 1 µL of 7.5 mg/ml protein solutions mixed with 1 µL of well solution containing 200 mM sodium citrate (pH 7.0) and 1.95-2.1 M ammonium sulfate. Selected crystals were transferred to a cryo-solution composed of the components of the reservoir with the addition of 15% glycerol, and diffraction data were collected on a home source Riguka XtaLAB Synergy-R system. The diffraction data were processed with Rigaku CrysAlis^{Pro} software and merged with Aimless as implemented in the CCP4 software suite.

Initial phases were determined by molecular replacement using CCP4 Phaser and coordinated of PD-L1 from RCSB PDB 5C3T. A partial model of the CDP was built in the resulting electron density difference maps. Iterative rounds of alternating positional refinement and model building, using the programs Refmac and COOT, included placing an N-linked glycan and ordered solvent molecules. Residues or side chains that did not exhibit $2F_{obs}$-F_{calc} electron density when contoured at 0.7σ were removed or truncated to the Cβ atom. The quality of the final model was assessed using ProCheck and Molprobity. The structure was deposited into RCSB as PDB 7SJQ.

Surface Plasmon Resonance (SPR) Interaction Analyses

SPR experiments were performed at 25°C on a Biacore T100 instrument (Cytiva) with a Series S SA chip and 10 mM HEPES, pH 7.4, 150 mM NaCl, 3 mM EDTA, 0.05% Tween 20 and 0.1 mg/mL bovine serum albumin (BSA) as the running buffer. Biotinylated human PD-L1-His-Avi (produced in-house but comparable to Acro PD1-H82E5) at 0.5 µg/mL (PDL1B1G1 assays) or 0.2 µg/mL (PDL1B1G2 and PDL1B1G-N22Q assays) in running buffer was injected at 10 µL/minute for various lengths of time to capture the RU amounts noted. All experiments used a blank streptavidin flow cell for referencing. PDL1B1G1 binding was performed on a captured PD-L1 surface with a density of 143 RUs. Serial 2-fold dilutions of PDL1B1G1 (2.4 µM to 600 pM) were injected in random order with a buffer blank every 5th injection and run in duplicate at a flow rate of 50 µL/minute with 2 minutes of association and 2 minutes of dissociation. Double-referenced data were fit with a steady-state 1:1 interaction model with BiaEvaluation 2.0.4 software. PDL1B1G2 and PDL1B1G2-N22Q assays were run with PD-L1 captured on 3 flow cells at different densities (32, 68 and 136 RUs) using a kinetic titration method. Three buffer blank cycles were run prior to each PDL1B1G2 cycle with the 2nd and 3rd buffer cycles averaged for double-referencing. PDL1B1G2 and PDL1B1G2-N22Q were each injected

sequentially at 0.02, 0.08, 0.31, 1.25, and 5 nM at 50 μL/minute for 7 minutes with a final dissociation of 20 minutes. Data from all surfaces were analyzed globally with a single cycle kinetic analysis model in BiaEvaluation 2.0.4 software. The data is partially mass transfer limited with reported rate constants $k_a = 1.25 \pm 0.01 \times 10^8$ $M^{-1}s^{-1}$, $k_d = 2.00 \pm 0.01 \times 10^{-2}$ s^{-1} and $k_t = 2.10 \times 10^8$ RU x $M^{-1}s^{-1}$ for PDL1B1G2 and $k_a = 9.73 \pm 0.06 \times 10^7$ $M^{-1}s^{-1}$, $k_d = 1.96 \pm 0.01 \times 10^{-2}$ s^{-1} and $k_t = 1.71 \times 10^8$ RU x $M^{-1}s^{-1}$ for PDL1B1G2-N22Q. Figures were made in Prism 9 for Mac OS software. SPR measurements are presented with error in the text and figures, but note that this error represents a precision estimate based on fitting residuals, rather than an accuracy estimate based on replicate measurements.

Histology

Paraffin-embedded tumors were sectioned at 4 μm, mounted (Fisherbrand 2155015), and stained using a Ventana Discovery Ultra IHC/ISH autostainer. Deparaffinization was followed by antigen retrieval (Ultra CC1, Roche 950-224) at 37°C for 32 mins (CD8) or 24 mins (Granzyme B). Using the ChromoMap DAB kit (Roche 760-159), sections were blocked, incubated with primary anti-CD8 antibody (Invitrogen MA514548, 1:25, 40 mins at 37°C) or anti-granzyme B antibody (Abcam, ab134933, 1:100 for 28 mins at 37°C), and detected with anti-rabbit HQ (Roche 760-4815) and anti-HQ-HRP (Roche 760-4820). Counterstaining used hematoxylin and bluing solution. Hematoxylin and eosin staining used Harris Hematoxylin (VWR 100504-402), bluing solution (VWR 95057-852) and 1% alcoholic Eosin Y (MilliporeSigma M117081100) before dehydrating, clearing, and mounting with MM24 (Leica 3801120).

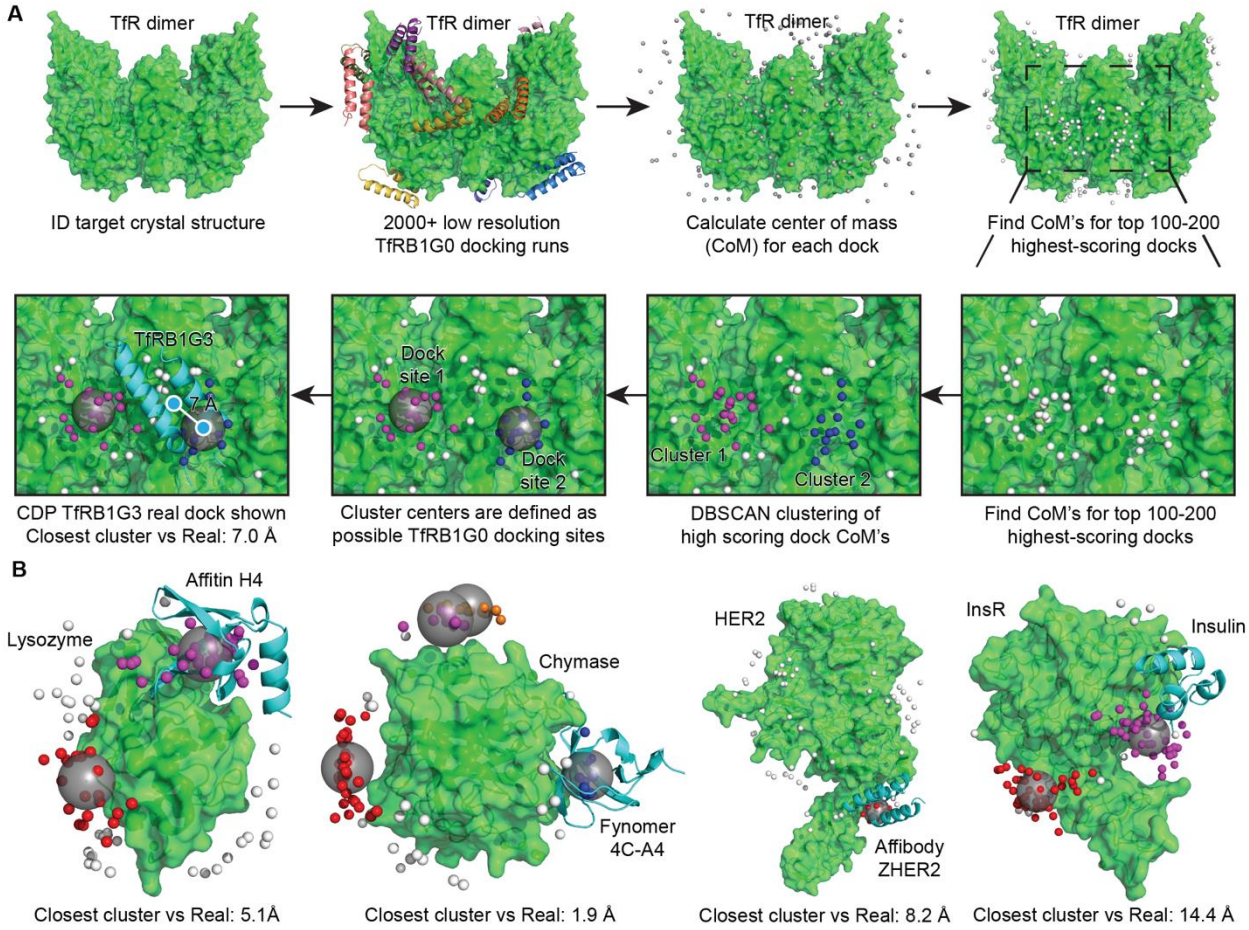

Fig. S1. Low-resolution RosettaDock clustering to identify possible miniprotein docking sites on a target structure. (A) Illustration of the docking site identification pipeline using a target (TfR) from a CDP:TfR co-crystal (PDB 6OKD); the CDP used for docking is the parent scaffold (TfRB1G0) of the high-affinity TfR-binding CDP (TfRB1G3) in the co-crystal. A target and CDP of interest are fed into RosettaDock in Low Resolution mode, performing at least 2000 runs. For each dock, the center of mass (CoM) of the CDP is identified and the docking interaction scored. The centers of mass from the top 100-200 docks are analyzed with DBSCAN to identify clusters of high-scoring docks (magenta or blue spheres for clusters 1 and 2, respectively), and the center of each cluster is defined as a possible miniprotein docking site, represented by a larger grey sphere. In this case, two possible docking sites were identified, one of which is within 7 Å of the real docking site (as measured using the CoM of TfRB1G3 in the co-crystal structure). **(B)** Four other miniprotein:target co-crystal structures were tested similarly, except the docked miniprotein was the co-crystal partner itself and not a model. Affitin H4:Lysozyme used PDB 4CJ2. Fynomer 4C-A4:Chymase used PDB 4AFS. Affibody ZHER2:HER2 used PDB 3MZW. Insulin:InsR used PDB 4OGA. The distance (in Å) between the closest docking site and the real CoM of the miniprotein in the co-crystal is shown below. Small spheres of a shared color are centers of mass within a given cluster. White small spheres are centers of mass from high-scoring docks that did not belong to a cluster using DBSCAN.

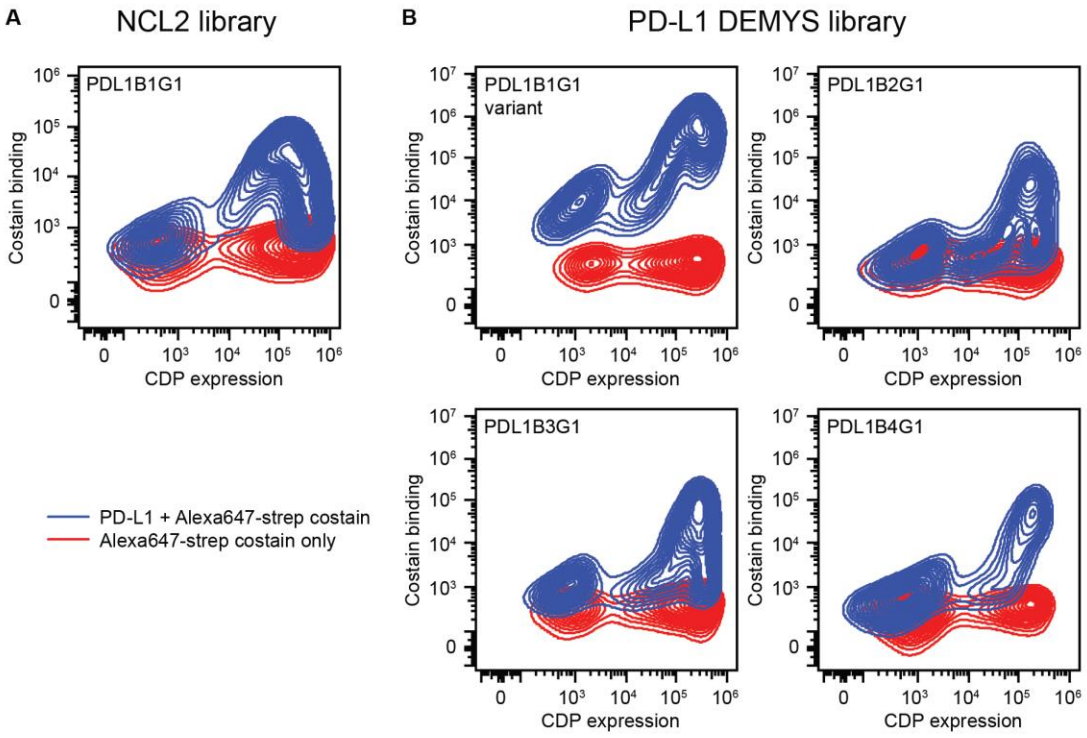

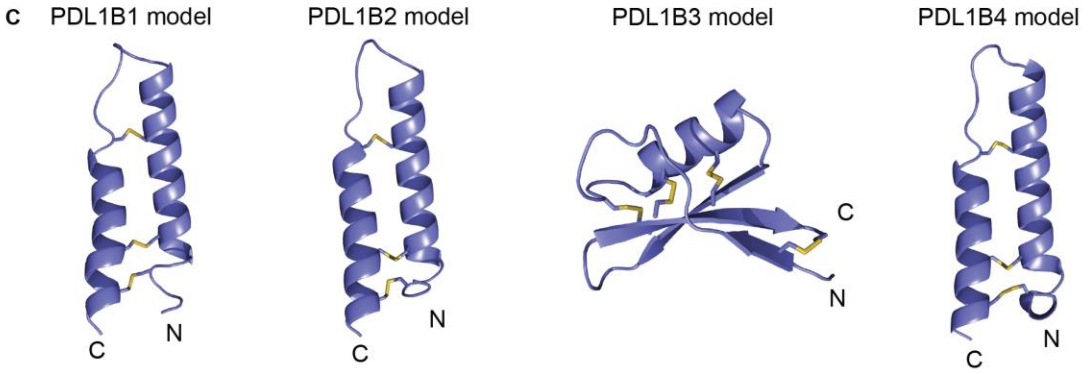

Binder	Gen	Sequence (Red = Mutated between parental and hit)	Cystine pairing*
PDL1B1	G0	EEDCKVHCVKEWAAYKACAERIKSDTTGQAHCSGQYFDFWKCVDHCAAP	C4–C46 C8–C42 C18–C32
	G1	EEDCKVHCVKEWAAYKACAERIKSYTIGRAHCSGQYFDVWKCLDHCAAP	
PDL1B2	G0	EESCKPQCVKAWLEYQACAERVEKDESGEAHCTGQYFDYWHCVDKCAAK	C4–C46 C8–C42 C18–C32
	G1	EESCKPQCVKAWLEYQACAERVEKDESGEAHCTGQYFDLWGCVDKCVAP	
PDL1B3	G0	ARTCESQSHRFKGPCVSDTNCASVCRTERFSGGHCRGFRRRCLCTKHC	C4–C48 C15–C35 C21–C42 C25–C44
	G1	ARTCESQSHRFKGPCVSDTMCASVCRTERFSGGHCRGFRRRCLCSKHC	
PDL1B4	G0	EERCKPQCVKSLYEYEKCVKRVENDDTGHKHCTGQYFDYWSCIDKCVAS	C4–C46 C8–C42 C18–C32
	G1	EERCMPQCVKSLYEYEKCLKRVENDDTGHKHCTGHYFDYWSCIDKCVAS	

Fig. S2. Flow plots (CDP expression vs. Costain fluorescence) for transiently transfected SDGF-cloned CDPs identified in PD-L1 mammalian display screening. (A) Single binder identified from NCL2 library screen. **(B)** Four clones representing distinct scaffolds identified from PD-L1 DEMYS library screen. PDL1B1G1 variant shares the same parental scaffold with the hit from NCL2. Costain is Alexa647-streptavidin. **(C)** I-TASSER/Rosetta models of the parent scaffolds for PD-L1 binders PDL1B1G1, PDL1B1G2, PDL1B1G3, and PDL1B1G4. In the table below, "Gen G0" is the parental scaffold with its sequence in the third column, while "Gen G1" is the hit itself. Their sequences are colored red where mutations differentiate the G1 hit from the G0 parent sequence. *: Only PDL1B1 had its cystine pairing confirmed by crystallography; the others are inferred by their I-TASSER/Rosetta models.

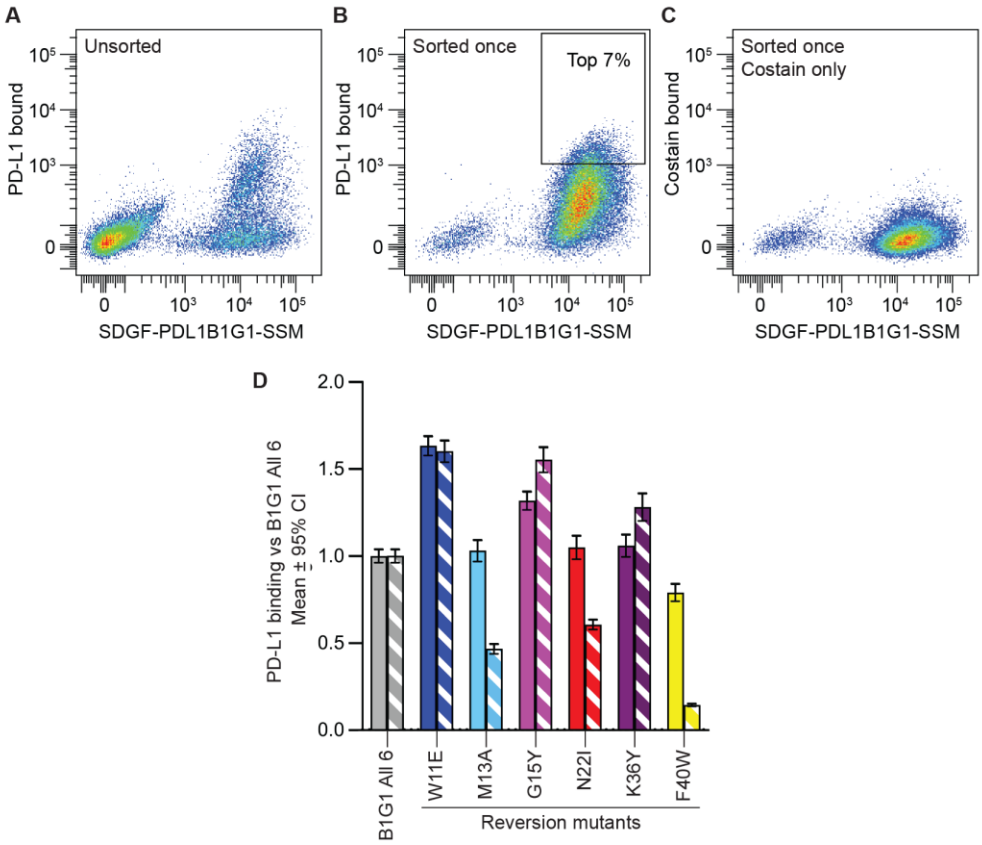

Fig. S3. Site-saturation mutagenesis of PDL1B1G1 and derivation of PDL1B1G2. (A to C) Flow cytometry plots of PD-L1-binding (streptavidin co-stain) of SSM library, either (A) unsorted, (B) sorted once, or (C) sorted once but with PD-L1 withheld in the stain. Top 7% gate in (B) represents cells that produced final enrichment data. **(D)** Six substitutions were identified in the SSM analysis as highly enriched. The all-6-substitutions variant (B1G1 All 6) was constructed, as were the six variants representing 5 of 6 substitutions, labeled with the reversion mutation from B1G1 All 6. Staining took place with either a 10 nM single-step stain (PD-L1 and streptavidin co-stain pre-incubated to produce tetrameric PD-L1 with high avidity) or a 50 nM two-step stain (PD-L1 incubated with cells before rinsing and streptavidin addition, representing monovalent PD-L1 binding). The latter stain can identify variants whose off-rates may be particularly hampered; see F40W for an example.

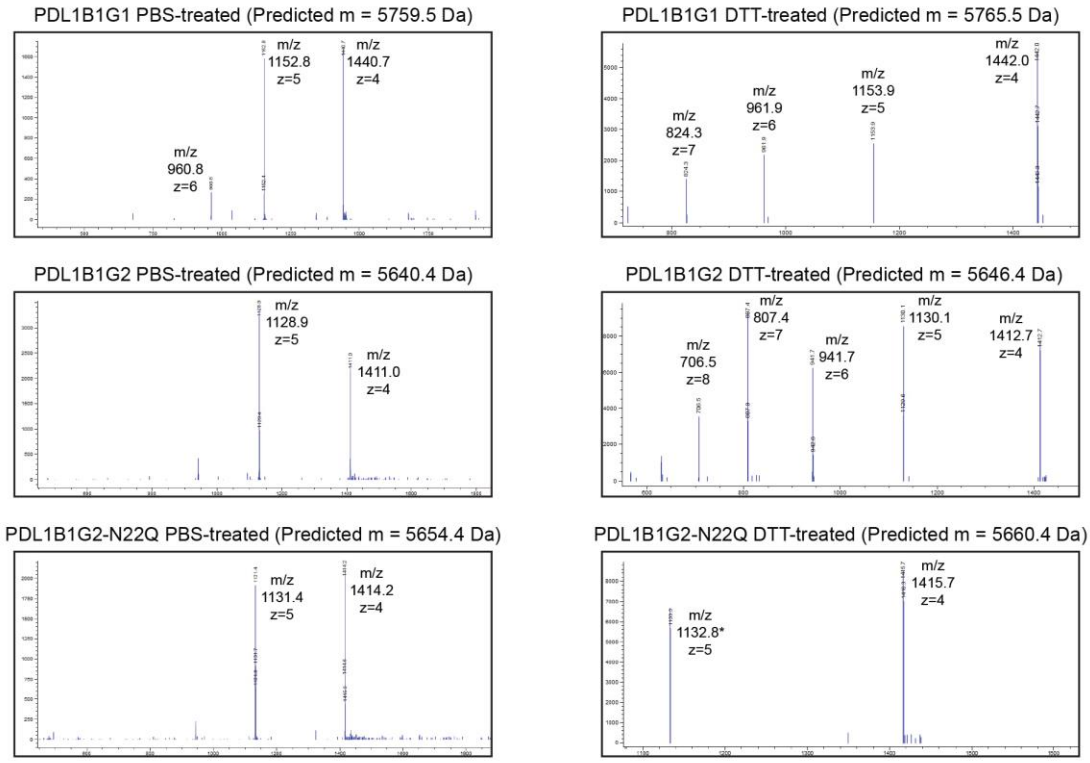

Fig. S4. Mass spectrometry traces of PD-L1-binding CDPs under native and reducing conditions. Native conditions involved resuspending lyophilized CDPs in PBS prior to LC-MS. Reducing conditions include 10 mM DTT with the PBS. Observed masses (average of observed [m/z * z – z]) had errors compared to Expasy predicted masses as follows: PDL1B1G1 PBS-treated, 110 ppm; PDL1B1G1 DTT-treated, 224 ppm; PDL1B1G2 PBS-treated, 115 ppm; PDL1B1G2 DTT-treated, 245 ppm; PDL1B1G2-N22Q PBS-treated, 354 ppm; PDL1B1G2 DTT-treated, 272 ppm. DTT treatment imparted apparent mass gains of 5.4, 5.3, and 6.5 Da for PDL1B1G1, PDL1B1G2, and PDL1B1G2-N22Q, respectively. *: A software error resulted in the most abundant PDL1B1G2-N22Q species in the z = 5 peak (m/z = 1132.8) being unlabeled in the exported image.

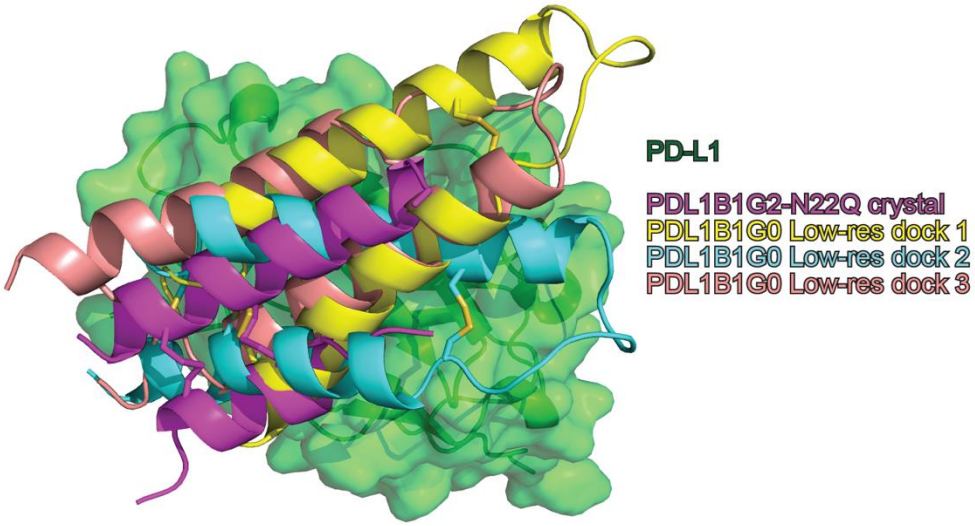

Fig. S5. Three low-resolution docking models of PDL1B1G2 parental scaffold. These were selected because their locations and orientations are similar to that of PDL1B1G2-N22Q shown in the crystal structure.

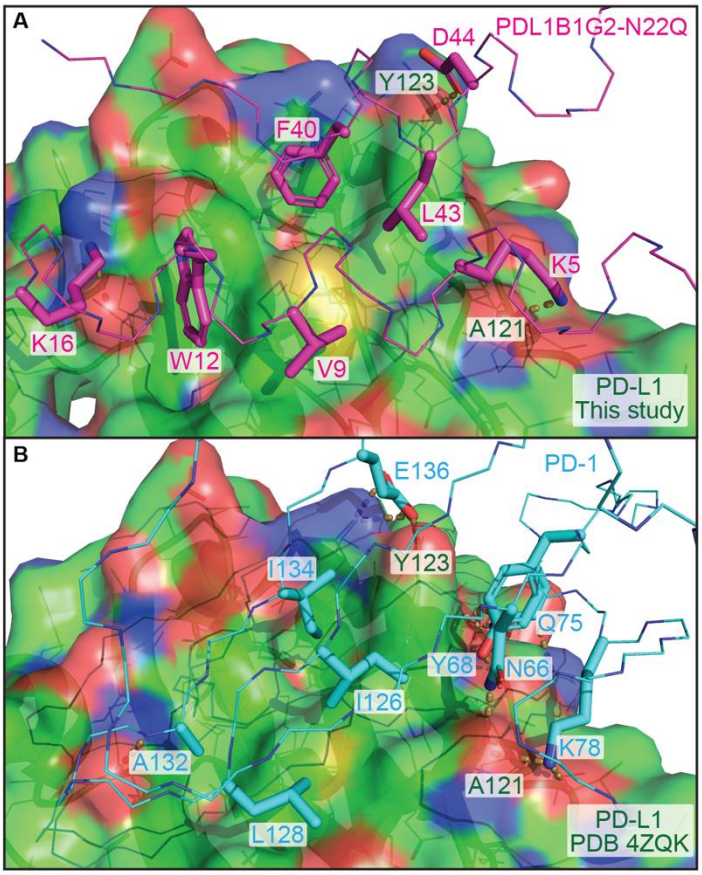

Fig. S6. Shared PD-L1 interactions between CDP and PD-1. (A) The CDP:PD-L1 co-crystal, where a wire diagram of PDL1B1G2-N22Q has side chains of interest as thick sticks. **(B)** The same but with PD-1 (from PDB 4ZQK). Sites of similar interactions are described in the main text. PD-L1 residues are in green text, PDL1B1G2-N22Q residues are in magenta text, and PD-1 residues are in cyan text.

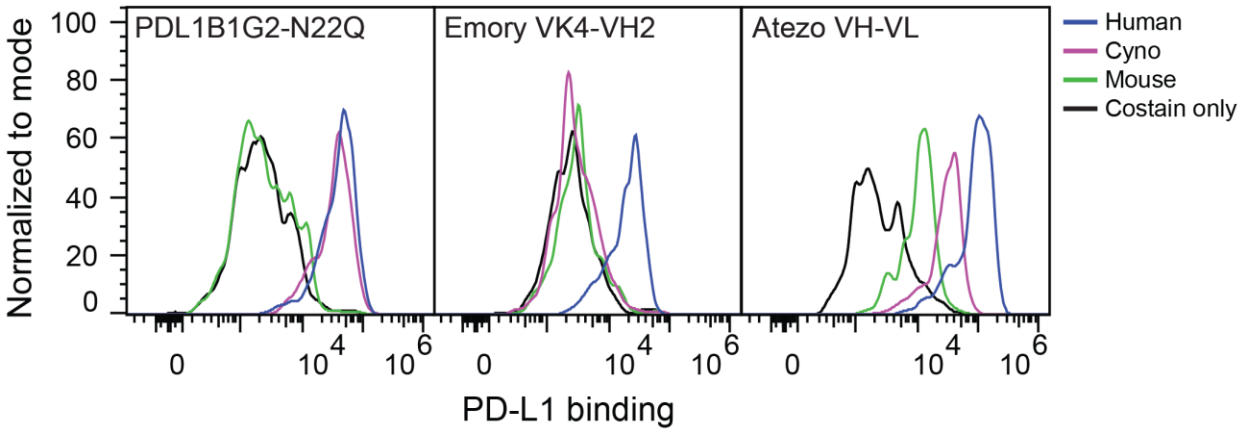

Fig. S7. Cells expressing surface-tethered (via SDGF) PD-L1 binding moieties and stained with various PD-L1 molecules. Surface-displayed molecules were CDP PDL1B1G2-N22Q, a VK-VH-formatted scFv derived from an anti-PD-L1 from Emory University (Emory VK4-VH2), and a VH-VL formatted scFv derived from the clinical anti-PD-L1 drug atezolizumab (Atezo VH-VL). Cells were stained with His-tagged human, cynomolgus, or mouse PD-L1 and anti-His-iFluor647 antibody, or anti-His-iFluor647 antibody alone. Co-stain fluorescence of cells is shown on the X-axis (APC channel). PDL1B1G2-N22Q demonstrates binding to both human and cynomolgus PD-L1 but no murine PD-L1 binding. Emory VK4-VH2 demonstrates binding to only human PD-L1. Atezo VH-VL demonstrates binding to all three. The scFv domains were of the described orientations with a $[GGGGS]_3$ linker joining VL/VK and VH domains.

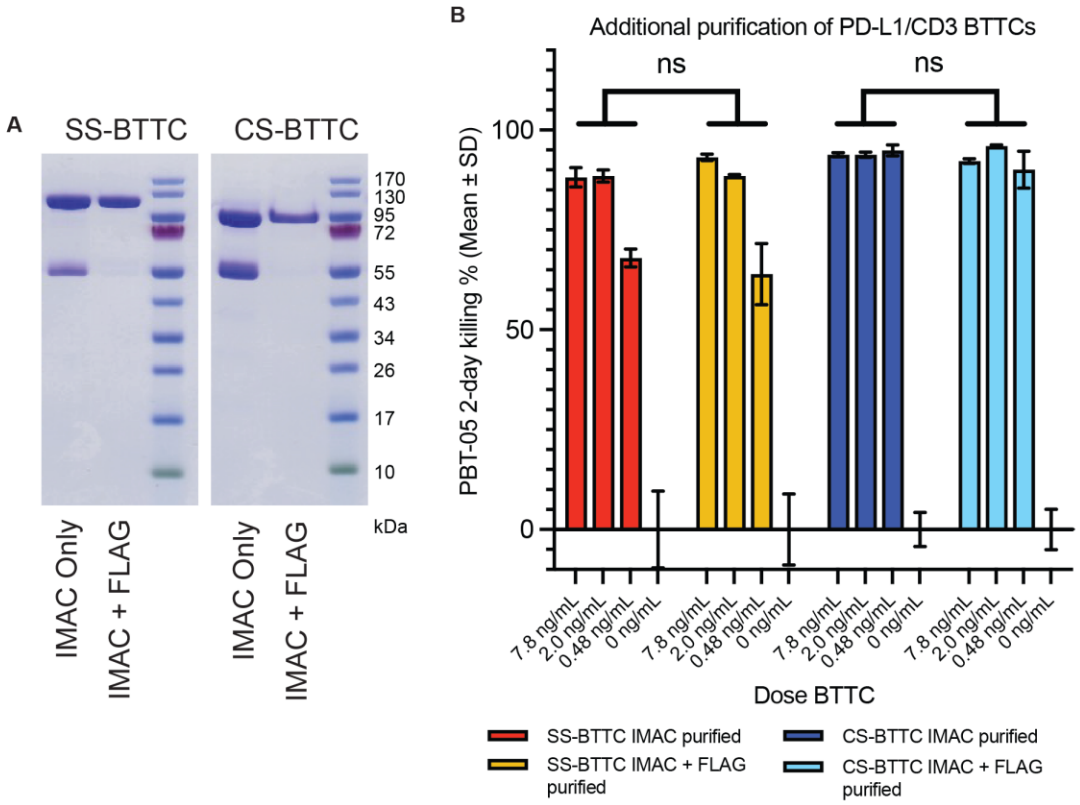

Fig. S8. PD-L1/CD3 Fc BTTCs CS-BTTC and SS-BTTC contained an inert low molecular weight impurity that represents monomeric anti-CD3-scFV-Fc. (A and B) The anti-CD3-scFv-Fc arm of the BTTC contains a 6xHis tag (permitting IMAC purification) but no FLAG tag, while the PD-L1-engaging arm of both BTTCs contains a FLAG tag. Small scale anti-FLAG M1 bead purification of the BTTCs away from the monomeric anti-CD3-scFv-Fc impurity **(A)** was followed by a repeat of the PBT-05 in vitro TCK assay **(B)**. Doses were normalized to BTTC concentrations only via densitometry quantitation. Lack of statistical significance (ns) in comparing IMAC with IMAC + FLAG purified performance was determined by Kolmogorov-Smirnov test.

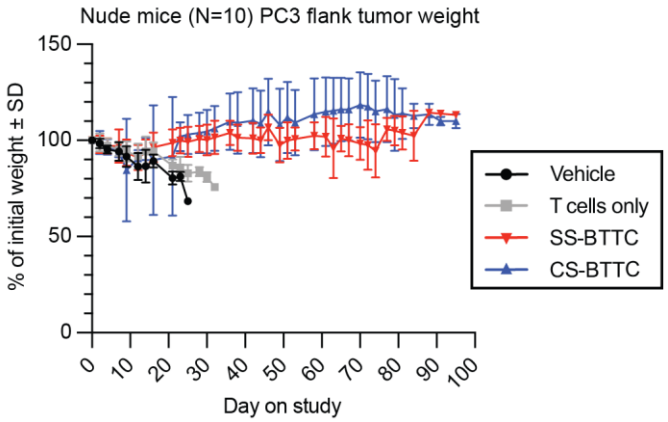

Fig. S9. PC3 subcutaneous flank tumor-bearing nude mice in cohort 1 demonstrated no difference in weight upon treatment with T cells only or T cells with either SS-BTTC or CS-BTTC. ns: over the first 12 days after enrollment (after which tumor-bearing mice began to show decline in health), all arm-vs-arm pairwise comparisons of cohort masses failed to show statistically significant differences by Mann-Whitney test.

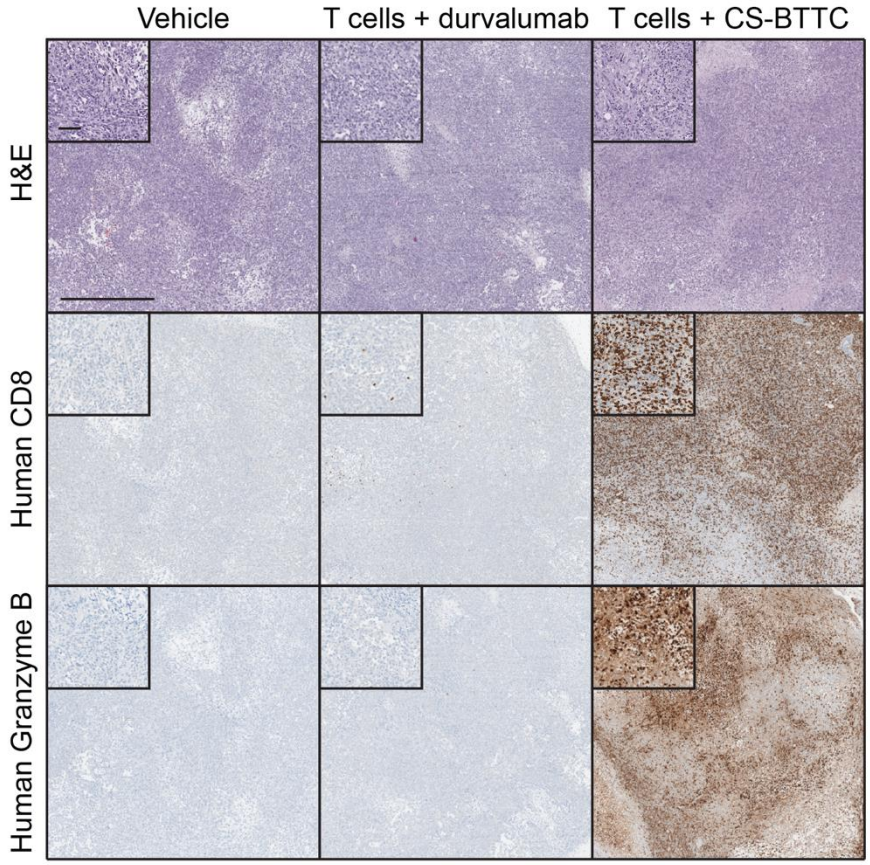

Fig. S10. Histology of PC3 tumors 14 days after treatment. Hematoxylin and eosin (H&E), human CD8, and human granzyme B staining of activated T cell infiltration in vehicle-, durvalumab, and CS-BTTC-treated tumors. Scale bar (top left panel): 100 μm in inset (5x objective), 1 mm in wide view (2x objective).

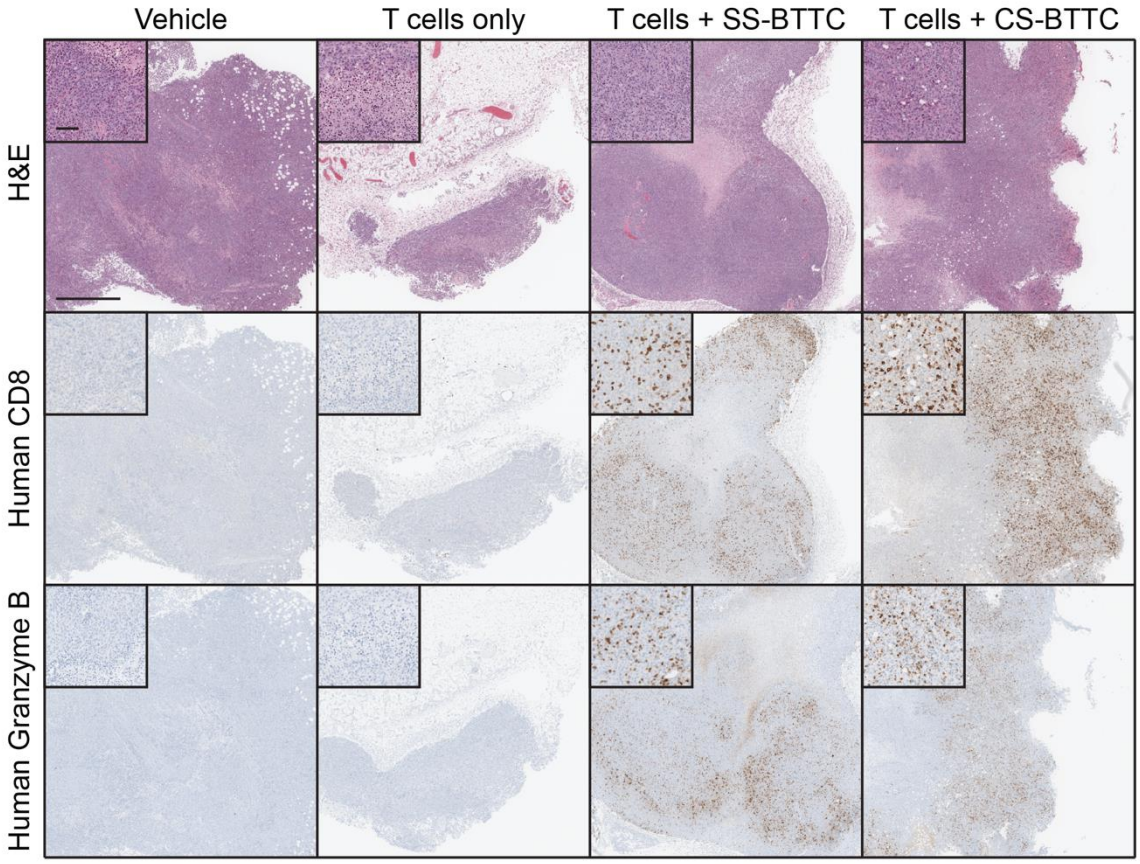

Fig. S11. Histology of MDA-MB-231 tumors 14 days after treatment. Hematoxylin and eosin (H&E), human CD8, and human granzyme B staining of activated T cell infiltration in vehicle, T cell-, SS-BTTC-, and CS-BTTC-treated tumors. Scale bar (top left panel): 100 μm in inset (5x objective), 1 mm in wide view (2x objective).

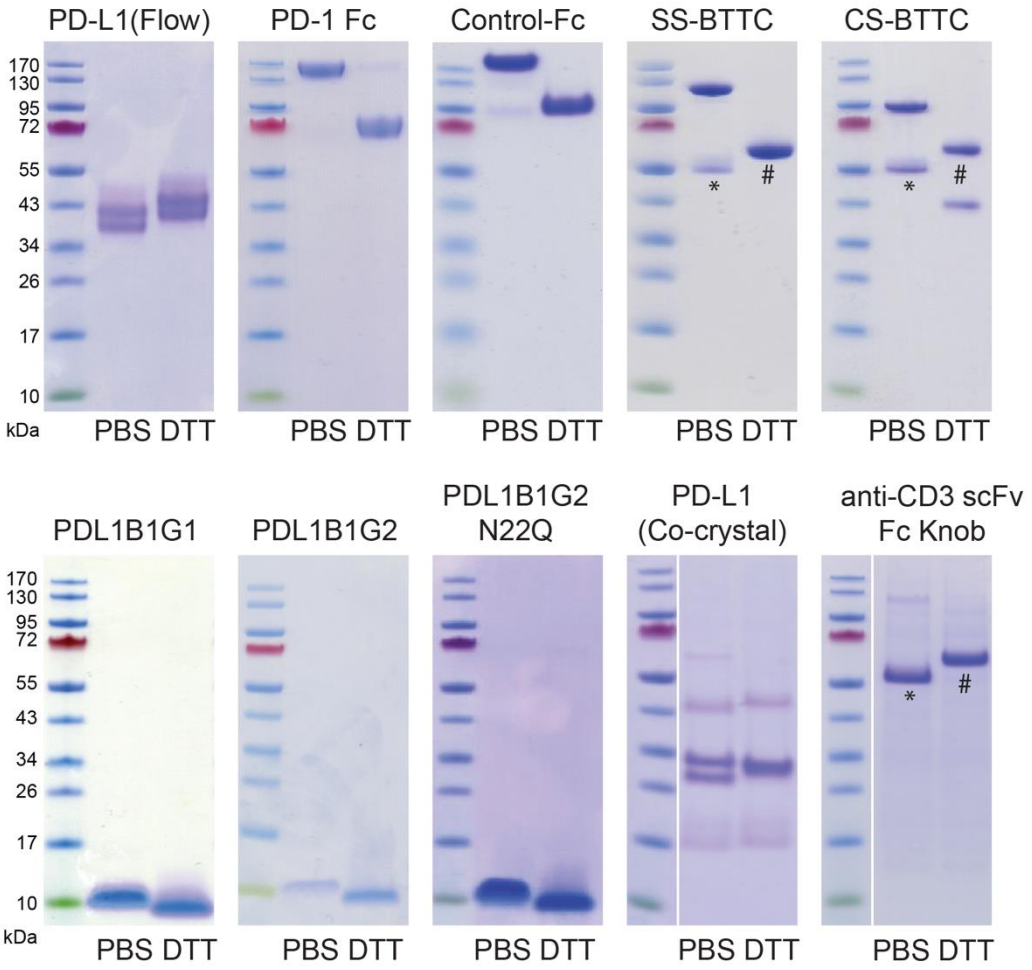

Fig. S12. Full SDS-PAGE gels of recombinant proteins used in this study. PBS/DTT: either PBS or 10 mM DTT (10% v/v) were included in LDS sample buffer prior to pre-gel boiling. PD-L1 for flow studies contained both extracellular Ig domains (F19-N238), while the co-crystallization reagent contained only the N-terminal Ig domain (A18-Y134). For both PD-L1 recombinant proteins, N-linked glycans were allowed to remain intact (i.e. were not mutated away). All Fc-containing proteins, including knob-and-hole BTTC molecules SS-BTTC and CS-BTTC, contain the IgG1 hinge region between the binder of interest (PD-1, control target, CDP, or scFv) and the Fc domain, which includes two cysteines that create a pair of interdomain disulfide bonds between the paired hinge regions (For example, see PDB 1HZH). This further stabilizes the dimer between the Fc domains in an SDS-stable fashion, which is why the Fc fusion proteins have drastically different mobility after DTT reduction. The exception to this is the anti-CD3 scFv Fc Knob protein expressed by itself (bottom right), which is not a disulfide-stabilized dimer as the knob mutations do not permit stable dimerization and resulting disulfide formation. "*" and "#" denote SDS-PAGE mobility of non-BTTC contaminants in SS-BTTC and CS-BTTC that correspond to monomeric anti-CD3 scFv Fc Knob.

Table S1: CDP crystallization data collection and refinement statistics.

PDB ID	7SGQ	7SLT	7SAO	7SNC	7SND	7SAP
Crystallization condition	0.2 M Li_2SO_4, 0.1 M Tris pH 8.5, 40 % PEG 400	0.2 M $CaCl_2$, 0.1 M Bis-tris pH 5.5, 45% MPD	5 mM $CoCl_2$, 5 mM $CdCl_2$, 5 mM $NiCl_2$, 0.1 M HEPES pH 7.2, and 12 % PEG 3350	0.2 M di-Sodium tartrate, 20% (w/v) PEG 3350	0.2 M LiCl, 0.1 M Phosphate Citrate pH 4.2, 20 % (w/v) PEG 1000	0.1 M MES pH 6.5, 25 % (w/v) PEG 8000
Data collection						
Space group	C 1 2 1	C 1 2 1	C 2 2 2_1	C 2 2 2_1	P 1 2_1 1	P 1 2_1 1
Cell dimensions						
a, *b*, *c* (Å)	65.8, 72.7, 41.2	33.9, 67.4, 50.4	33.16, 78.08, 27.73	31.1, 80.3, 28.4	26.1, 52.2, 35.1	19.8, 50.5, 25.3
α, β, γ (°)	90.0, 123.1, 90.0	90.0, 108.9, 90.0	90.0, 90.0, 90.0	90.0, 90.0, 90.0	90.0, 101.3, 90.0	90.0, 104.5, 90.0
Resolution (Å)	50.00 - 2.09 (2.13 – 2.09)	50.00 - 1.95 (1.98 - 1.95)	50.00 – 1.78 (1.84 – 1.78)	50.00 – 2.10 (2.14 – 2.10)	50.00 - 1.80 (1.86 - 1.80)	50.00 - 1.79 (1.85 - 1.79)
R_{merge}	0.13 (0.49)	0.08 (0.41)	0.05 (0.15)	0.04 (0.08)	0.07 (0.16)	0.03 (0.18)
R_{meas}	0.14 (0.59)	0.11 (0.51)	0.05 (0.19)	0.04 (0.08)	0.07 (0.18)	0.04 (0.18)
$I/\sigma(I)$	12.64 (1.58)	29.9 (1.77)	30.54 (2.24)	51.80 (25.90)	49.80 (7.52)	35.6 (3.1)
$CC_{1/2}$	-0.82	-0.93	-0.99	-0.99	-0.96	-1
Completeness (%)	95.6 (58.3)	89.9 (37.5)	80.6 (5.2)	100 (92.7)	100 (74)	98.5 (6.2)
Redundancy	6.7 (2.9)	6.6(2.8)	6.3 (1.2)	6.6 (5.1)	7.2 (3.5)	3.3 (1.8)
Refinement						
Resolution (Å)	27.58 - 2.09 (2.14 - 2.09)	28.98- 2.00 (2.05 – 2.00)	22.61 – 1.78 (1.84 – 1.78)	23.21 – 2.10 (2.17 – 2.10)	28.75 - 1.79 (1.84 - 1.79)	25.25 - 1.79 (1.85 - 1.79)
No. reflections	8919 (470)	6489 (257)	3176 (76)	2263 (220)	6003 (68)	3164 (38)
R_{work} / R_{free}	0.2ccp45/0.32	0.20/0.23	0.21/0.26	0.21/0.25	0.14/0.21	0.14/0.18
No. atoms						
Protein	1268	910	264	264	980	490
Ligand/ion	0	0	0	0		
Sulfate	10					12
Phosphate					5	

Glycerol		18			12	
Water	33	52	23	28	88	57
B factors						
Protein	33.7	38.7	17	24.47	35.02	40.12
Ligand/ion	30.7	40.6	0	0	44.74	0
Water	48.8	55.5	27.68	30.68	26.17	28.21
R.m.s. deviations						
Bond lengths (Å)	0.009	0.01	0.009	0.014	0.009	0.017
Bond angles (°)	1.85	1.72	1.81	1.18	1.631	1.79

[a]Values in parentheses are for highest-resolution shell.

Table S2: PDL1B1G2-N22Q:PD-L1 data collection and refinement statistics. Numbers in Parentheses are for reflections in highest resolution shell.

PDB ID	7SJQ
Data Collection	
Space Group	C 2 2 2_1
Cell Dimensions a, b, c (Å)	56.0, 65.3, 99.9
Resolution Range (Å)	50.00-2.00 (2.07-2.00)
Wavelength (Å)	1.54
Unique Reflections	12732 (1272)
Completeness (%)	99.8 (99.5)
Average Redundancy	4.6 (3.7)
Rmerge (%)	3.9 (15.4)
I/σ(I)	32.5 (8.3)
Structure Refinement	
Resolution (Å)	50.00-2.00
No. of Reflections	
all/test	12119/593
No. of non-hydrogen atoms (average B-factor (Å2))	
Protein	1186 (55.0)
others (solvent)	103 (31.9)
Rcryst/Rfree (%)	18.5/23.2
Rmsd Bonds (Å)/Angles (°)	0.011/1.618
Estimate of Coordinate Error (Å) Maximum likelihood e.s.u.	0.097
Ramachandran values (ProCheck)	
Favored region (%)	90.3
Allowed region (%)	9.7
Outlier region (%)	0
Molprobity percentile (score)	100 (1.04)